# A experimental study of I-II-III mixed mode crack fracture of rock under different temperature

**LI Li-yun**[1, *], **XU Zhi-qiang**[1], **LI Ming-xiu**[1], **LIU Yi**[1], **FAN Chen**[1], **TANG Tie-Wu**[1], **LIU Da-an**[2]

[1]China University of Mining and Technology, Beijing 100083, China;
[2]Institute of Geology and Geophysics, Chinese Academy of Science, Beijing 100029, China
[*] Corresponding author: lly@cumtb.edu.cn

**Abstract** A series of critical fracture toughness of two kinds of rock materials under different temperature which varied from -50°C to 240 °C are measured by I-II-III mixed mode fracture experiments adopting atypical three point bending specimens. Relative stress intensity factors of crack initiation are calculated by finite element method. Combining with calculated values, the experiment result shows that, the mixed mode fracture toughness of the rocks decreases with the increase of temperature. The experimental and calculated results can be used in the design of deep underground engineering and disaster prevention and mitigation engineering。

**Key words** rock crack fracture, I-II-III mixed mode , temperature, experiments, finite element method.

## 1. Introduction

The rock mass whole structure failure in underground engineering is the process of damage, crack fracture and propagation. Deep mining engineering and geological disposal engineering such as nuclear waste, carbon dioxide and garbage deeply buried belong to the underground geotechnical engineering combining with temperature variation. Therefore, the investigation of the propagation behavior of rock crack under different temperature will be very important. Preliminary studies on temperature effect are mainly concentrated in mode I rock crack[1-3], a small amount of studies are concentrated in mixed-mode I-II rock crack[4-7]. About three-dimensional propagation behavior of rock crack which containing mode III stress intensity factor, the authors have done some researches under the room temperature in the recent time [8-9]. But the research about mixed mode I-II-III rock crack fracture coupling with temperature effect, there is almost no published paper, but it has important significance in deep underground engineering, for this mixed mode crack coupling with temperature is the basic existence in deep underground engineering. Consider of this, three point bending I-II-III mixed mode fracture experiments of two kinds of granite were carried out under 6 temperature levels in this paper. The variation law of critical fracture load v.s. temperature was measured. Combined with finite element method (FEM) calculation, the stress intensity factors in crack tip line under the critical load were got. The results of the paper both in experiments and in numerical calculation can provide a valuable reference for the deep underground engineering design and disaster prevention engineering design.

## 2. Experimental investigation

## 2.1. Preparation of specimen

The rocks used in this experiment investigation are two kinds of granite: white linen granite and red linen granite. They have different grain sizes. The grain size of the former is smaller than later. Specimen contours are both 140mm×40mm×24mm (Figure 1). From specimen central section, in the position $L$=15mm and $L$=30mm, an edge crack which width is not more than 1mm were cut by diamond wheel blade. Crack length $a$＝20mm.

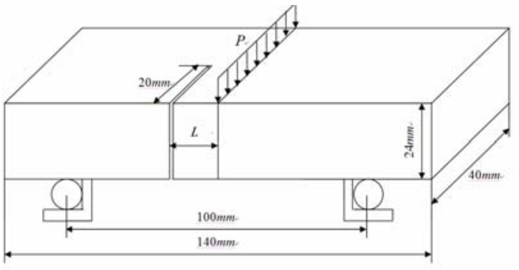


Figure 1 Specimen diagram and loading mode

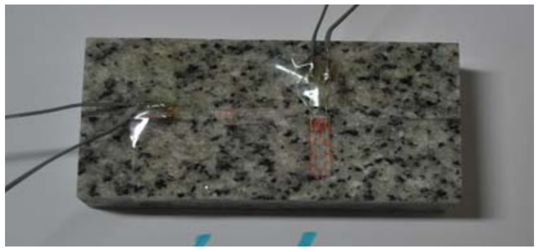

Figure 2 Uniaxial compression experiment specimen

## 2.2. The process of experiment

For the finite element method (FEM) calculation subsequently in this paper, the elastic modulus of two rocks under different temperature was measured by uniaxal compression experiments. The contour of uniaxal compression specimen and test situation is shown in Figure 2 and Figure 3. The elastic modulus E measured under different temperature are listed in Table 1. Due to the difficulty of test technique，the Poisson's ratio of the two rocks under different temperatures were not measured except under ambient temperature. And then, about the variation law of Poisson’s ratio in different temperature was not mentioned in published documents. So in this paper Poisson’s ratio are assumed that it has no change when temperature changes; and it is measured under ambient temperature that: for white linen granite $\mu$ = 0.26 and for red linen granite $\mu$ = 0.3.

The loading way of abnormal three point bending test is shown in Figure 1. The experimental situation is shown in Figure 4. For the two kinds of granite, under different temperature and different crack position L, the critical fracture loads F measured by experiments are listed in Table 2.

Table 1 ：Elastic modulus E of two kinds of granite under different temperatures

| Type of specimen | Elastic modulus $E$/GPa | | | | | |
|---|---|---|---|---|---|---|
| | -50$^0$C | -25$^0$C | Room temperature | 80$^0$C | 160$^0$C | 240$^0$C |
| White linen granite | 18.8685 | 17.643 | 15.3455 | 17.1 | 18.3985 | 17.087 |
| Red linen granite | 17.033 | 15.992 | 17.713 | 17.56 | 17.9665 | 19.196 |

Whether in high temperature test or in low temperature test, before a test, the specimen must be placed in the oven in which temperature has arrived demand level half an hour in order to get a well-distributed temperature within specimen. In the experimental process, the loading way of test machine was controlled by displacement. Loading rate is 0.015mm/min. In experiment it can be observed that the crack tip point at the bottom of the specimen starts fracture, it leads the specimen failure. The fracture section of specimen is not a plane, and presents a three-dimensional morphology. The failure pattern of the specimen is shown in Figure 5. The critical fracture loads under different temperature are shown in Table 2. The relative variation rate $\eta$ which was compared with the critical fracture load under ambient temperature, the values of $\eta$ v.s. temperature are listed in Tab. 3. $\eta$ is defined as:

$$\eta=(F-F_0)/F_0 \tag{1}$$

$F_0$ and $F$ are the critical fracture load under ambient temperature level and other temperature levels. $\eta$ can reflect the deviation extent between $F$ and $F_0$ under different temperature.

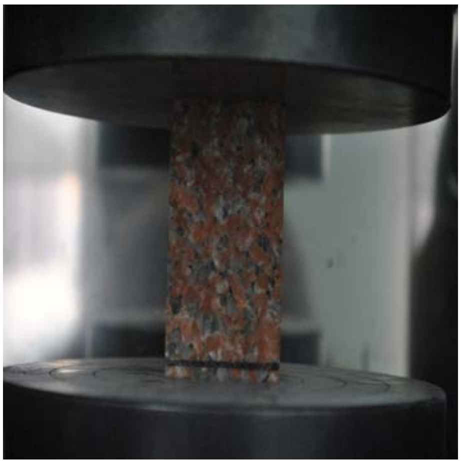

Figure 3 Uniaxial compression test

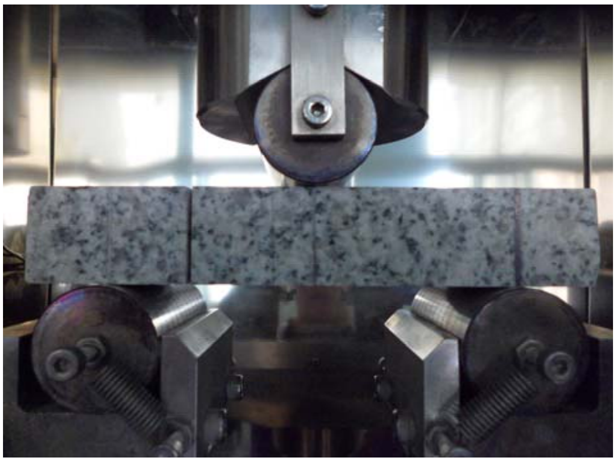

Figure 4 Abnormal three point bending experiment

Table 2 The critical fracture load $F$ v.s. temperature

| Type of specimen | Distance from the central position/mm | The critical fracture load $F$/（kN） | | | | | |
|---|---|---|---|---|---|---|---|
| | | $-50^0$C | $-25^0$C | Room temperature | $80^0$C | $160^0$C | $240^0$C |
| White linen granite | $L$=30 | 2.67 | - | 2.07 | 2.01 | 1.71 | 1.62 |
| | $L$=15 | 1.47 | 1.51 | 1.25 | 1.17 | 1.06 | 0.84 |
| Red linen granite | $L$=30 | 2.35 | 1.90 | 1.72 | 1.27 | 0.95 | 0.97 |
| | $L$=15 | 1.55 | 1.21 | 1.21 | 1.42 | 0.99 | 0.75 |

Table 3 The deviation rate $\eta$ between $F$ and $F_0$ under different temperature.

| Temperature /$^0$C | White linen granite | | Red linen granite | |
|---|---|---|---|---|
| | $L$=30mm | $L$=15mm | $L$=30mm | $L$=15mm |
| $-50^0$C | 28.95% | 17.86% | 37.02% | 27.95% |
| $-25^0$C | - | 21.10% | 10.61% | -0.47% |
| Room temperature | 0 | 0 | 0 | 0 |
| $80^0$C | -2.86% | -6.20% | -26.02% | 17.28% |
| $160^0$C | -17.32% | -15.12% | -44.53% | -18.25% |
| $240^0$C | -21.71% | -33.07% | -43.39% | -37.82% |

**2.3. The relationship between parameters and temperature**

It can be seen from Table 1 that in the range of -50$^{0}$C to 240$^{0}$C, with the temperature increases, the variation of elastic modulus $E$ is not obvious. It has only a little volatility.

From Table 2, for the same type of specimen, It can be seen that the critical fracture load reduce with the temperature increase. It is unconcerned with the crack location and the type of rock. Under the same temperature, the value of the critical load is related with the crack position. The shorter the distance between crack and central position of the specimen is, the lower the critical load is.

In the rang of -50$^{0}$C to 240$^{0}$C, for different specimens, with the temperature increase, the deviation rate η between $F$ and $F_0$ gradually reduce. For white linen granite, when $L$ = 30 mm, $\eta$ gradually reduce from 28.95% down to -21.71%. when $L$ = 15 mm, $\eta$ gradually reduce from 17.86% down to -33.07%. For red linen granite, when $L$ = 30 mm, $\eta$ gradually reduce from 37.02% down to -43.39%. When $L$ = 15 mm, $\eta$ gradually reduce from 27.95% down to -37.82%.

Figure 5 Specimen after fracture

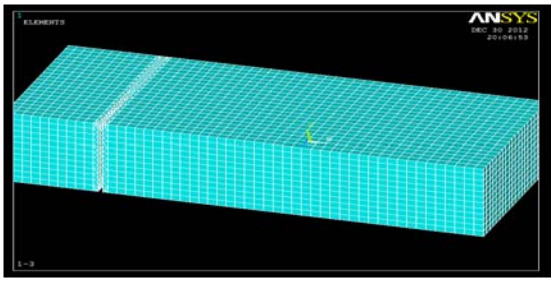


Figure 6 Divide grid

## 3. Finite element analysis

For abnormal three point bending I-II-III mixed mode fracture specimens in this paper, numerical solution of stress intensity factors for every point in crack tip line were not got in other documents, no more than analytic solutions. In this paper the distribution laws of stress intensity factors $K_{\mathrm{I}}$、$K_{\mathrm{II}}$、$K_{\mathrm{III}}$ and their critical values in crack fracture initiation point were obtained by FEM calculation under different temperatures.

### 3.1.Finite element modeling

By try of FEM calculations many times, it had been known that if the short sections outside the two lower supports of the specimen were ignore, it did not affect the simulation results obviously, so in this paper, the sections between the two lower supports of specimen were choose into FEM calculation. By this modeling way, unnecessary elements can be reduced. It can improve the calculation speed. Cartesian coordinate system was defined as follows: X axis is along the length of the specimen, Y axis is up along the specimen thickness direction, Z axis is forward along the width direction (Figure 6). The width of edge crack is not more than 1mm. The crack surface is a free surface, and the crack front is a rectangular shape. It is consistent with the crack front in the specimens of experiments. Scanning grid division is used. In order to get accurate stress values near crack tip, refined grids around crack tip are also used. Divided elements situation are shown in Figure 6. Substitute the material parameters $E$, $\mu$ and critical load $F$ into the FEM program, critical values (mixed mode critical fracture toughness) of $K_{\mathrm{I}}$, $K_{\mathrm{II}}$, $K_{\mathrm{III}}$ in failure crack tip can be calculated.

**3.2. The relation between stress intensity factors of initiation points and temperatures**

After the stress field calculated within the specimens by the finite element method, the three formulas following can be directly applied to calculate the stress intensity factors of the crack tip[10-11]:

$$K_{\mathrm{I}} = \lim_{r \to 0} \sqrt{2\pi r}\sigma_x \quad (2)$$

$$K_{\mathrm{II}} = \lim_{r \to 0} \sqrt{2\pi r}\tau_{xz} \quad (3)$$

$$K_{\mathrm{III}} = \lim_{r \to 0} \sqrt{2\pi r}\tau_{xy} \quad (4)$$

$r$ is the short distance from stress point to the crack tip

Put $r$ values and stress values of every point on crack extension cord into the formulas, and drew a straight line of $K_{\mathrm{I}}$、$K_{\mathrm{II}}$、$K_{\mathrm{III}}$ v.s. $r$, through the straight line, the real values of $K_{\mathrm{I}}$、$K_{\mathrm{II}}$、$K_{\mathrm{III}}$ can be got at the point $r = 0$[10-11].

In abnormal three point bending experiments (Figure 4), the crack fracture just initiated from the tension point which was on the crack tip point located on the bottom of specimen (Figure 4), so the relations between critical stress intensity factors and temperatures are listed in Table 4 and Table 5, and shown in Figure 7 to Figure 10.

Table 4 Critical stress intensity factors v.s. temperature (white linen granite)

| Temperatures | $L$=30mm | | | $L$=15mm | | |
|---|---|---|---|---|---|---|
| | $K_{\mathrm{I}}$/MPam$^{1/2}$ | -$K_{\mathrm{II}}$/MPam$^{1/2}$ | -$K_{\mathrm{III}}$/MPam$^{1/2}$ | $K_{\mathrm{I}}$/MPam$^{1/2}$ | -$K_{\mathrm{II}}$/MPam$^{1/2}$ | -$K_{\mathrm{III}}$/MPam$^{1/2}$ |
| -50$^0$C | 2.285 | 0.453 | 0.248 | 2.114 | 0.258 | 0.148 |
| -25$^0$C | - | - | - | 2.172 | 0.265 | 0.152 |
| Normal temperature | 1.772 | 0.351 | 0.180 | 1.794 | 0.219 | 0.126 |
| 80$^0$C | 1.721 | 0.341 | 0.186 | 1.682 | 0.205 | 0.118 |
| 16$^0$0C | 1.465 | 0.290 | 0.159 | 1.522 | 0.186 | 0.107 |
| 24$^0$0C | 1.387 | 0.275 | 0.150 | 1.200 | 0.147 | 0.084 |

Table 5 Critical stress intensity factors v.s. temperature (red linen granite)

| Temperatures | $L$=30mm | | | $L$=15mm | | |
|---|---|---|---|---|---|---|
| | $K_{\mathrm{I}}$/MPam$^{1/2}$ | -$K_{\mathrm{II}}$/MPam$^{1/2}$ | -$K_{\mathrm{III}}$/MPam$^{1/2}$ | $K_{\mathrm{I}}$/MPam$^{1/2}$ | -$K_{\mathrm{II}}$/MPam$^{1/2}$ | -$K_{\mathrm{III}}$/MPam$^{1/2}$ |
| -50$^0$C | 2.014 | 0.399 | 0.218 | 2.229 | 0.272 | 0.156 |
| -25$^0$C | 1.626 | 0.322 | 0.176 | 1.734 | 0.212 | 0.121 |
| Normal temperature | 1.470 | 0.291 | 0.159 | 1.676 | 0.205 | 0.117 |
| 80$^0$C | 1.318 | 0.261 | 0.143 | 2.043 | 0.249 | 0.143 |
| 160$^0$C | 0.816 | 0.162 | 0.088 | 1.218 | 0.149 | 0.085 |
| 240$^0$C | 0.794 | 0.157 | 0.086 | 1.083 | 0.132 | 0.076 |

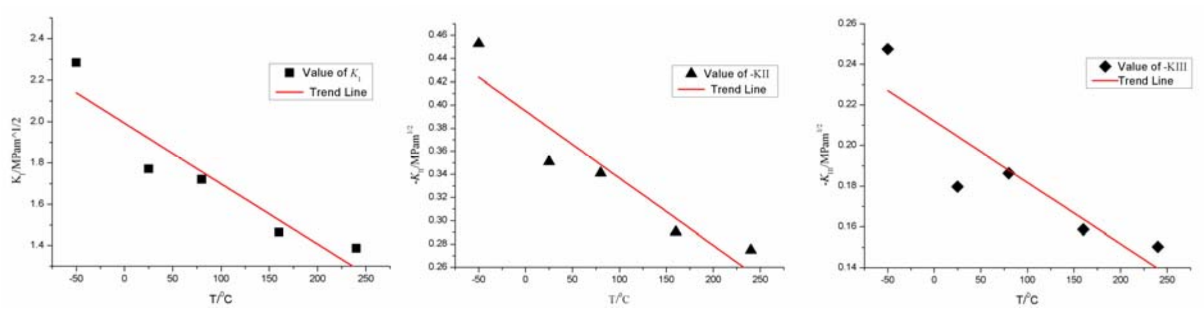


(a) Curves of $K_{I}$ (b) Curves of -$K_{II}$ (c) Curves of -$K_{III}$

Figure 7 The critical stress intensity factors v.s. temperature (white linen granite, $L$ =30mm)

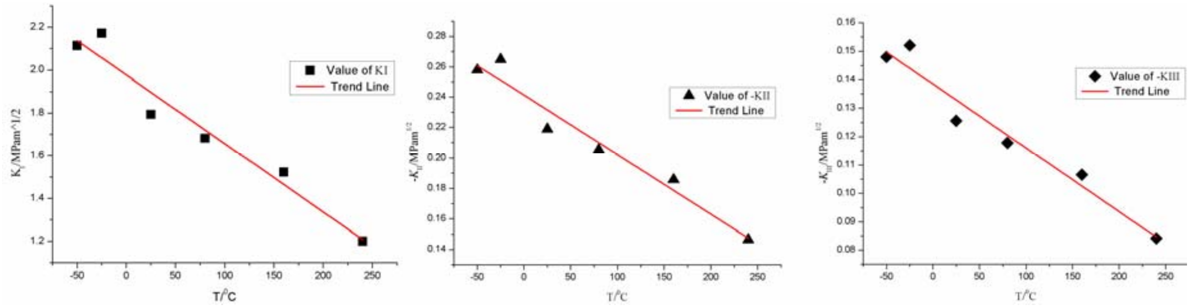


(a) Curves of $K_{I}$ (b) Curves of -$K_{II}$ (c) Curves of -$K_{III}$

Figure 8 The critical stress intensity factors v.s. temperature (white linen granite, $L$ =15mm)

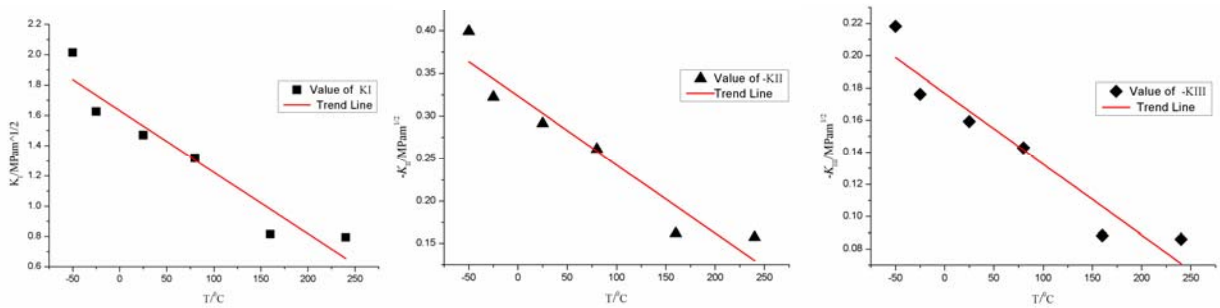


(a) Curves of $K_{I}$ (b) Curves of -$K_{II}$ (c) Curves of -$K_{III}$

Figure 9 The critical stress intensity factors v.s. temperature (red linen granite, $L$ =30mm)

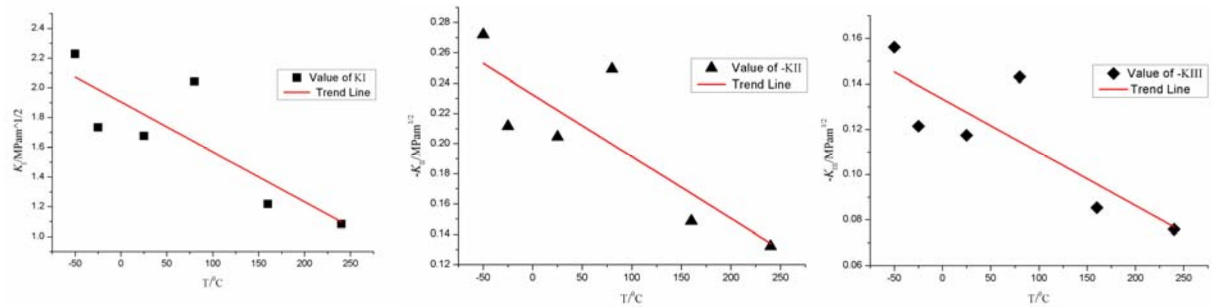


(a) Curves of $K_{I}$ (b) Curves of -$K_{II}$ (c) Curves of -$K_{III}$

Figure 10 The critical stress intensity factors v.s. temperature (red linen granite, $L$ =15mm)

## 3.3.Result analysis

From the Figures above， it can be seen that the absolute values of critical stress intensity factors decrease with the temperature increase. It is unconcerned with rock type and crack positions *L*. The reason is the critical fracture loads decrease with the temperatures increase, so the critical stress intensity factors $K_{\mathrm{I}}$、 $K_{\mathrm{II}}$、 $K_{\mathrm{III}}$ decrease relevantly.

From the Tab. 4 and Tab. 5, it can be seen that the $K_{\mathrm{I}}$ (>0) values at the initiation points for *L*=30mm specimen are generally smaller than the $K_{\mathrm{I}}$ (>0) values for *L*=15mm specimen. And the critical loads of the former are generally bigger than the latter. From this it can be known that, let the *L*=30mm specimen failure is more difficult than let the *L*=15mm specimen failure. But the relevant absolute values $K_{\mathrm{II}}$ and $K_{\mathrm{III}}$ of former are bigger than latter. It shows that, if $K_{\mathrm{I}}$ value who dominates the crack fracture initiation is not big enough, a I-II-III mixed mode rock crack tip can begin to expand, it has to have bigger $K_{\mathrm{II}}$ and $K_{\mathrm{III}}$ values. This result reflects a comprehensive effect of mixed mode rock crack fracture sufficiently.

## 4. Conclusion

(1) In the range of -50$^0$C to 240$^0$C, with the increase of temperature, the variation of elastic modulus *E* of two kinds of granite is not obvious; i.e. *E* values had no obvious differences between ambient temperature and some other temperature levels.

(2) For the same kind of rock crack specimen, with the increase of temperature, the critical fracture load is gradually reduced. The deviation rate $\eta$ decrease gradually from ( 20% to 40% ) under -50$^0$C to ( -20% to -40%) under 240$^0$C, i.e. at the lower temperature -50$^0$C, the crack initiation load will be higher ( 20% to 40% ) than at ambient temperature; at the higher temperature +240$^0$C, the critical fracture load will be lower ( 20% to 40% ) than at ambient temperature .

(3) For the same specimen, the critical stress intensity factor $K_{\mathrm{I}}$, $K_{\mathrm{II}}$, $K_{\mathrm{III}}$, at the crack fracture point, decrease with the temperature increase.

(4) At the same temperature, the longer the distance between crack and center of the specimen, the value of $K_{\mathrm{I}}$ (caused by tensile stress) in crack fracture point will be lower; and the critical load will be higher. It reflects the rock crack fracture initiation is mainly caused by tensile stress. If the $K_{\mathrm{I}}$ value is smaller, is the higher absolute value of $K_{\mathrm{II}}$, $K_{\mathrm{III}}$ at crack fracture initiation point required. It reflects the comprehensive effects in I-II-III mixed mode rock crack fracture.

**Acknowledgements**

This study is financially supported by Natural Science Foundation of China (No: 41072242) and National Basic Research Program under Grant No. 2010CB226802, 2011CB201201.

**References**

[1] Xu Xiaoli , Gao Feng , Ji Ming. Damage Mechanical Analysis of Fracture Behavior of Granite Under Temperature[J]. Journal of Wuhan University of Technology, 2010, 32(1):143-147.

[2] T Funat su, M Seto, H Shimada, et al. Combined effects of increasing temperature and confining pressure on the fracture toughness of clay bearing rocks[J]. International Journal of Rock Mechanics and Mining Sciences, 2004, 41(6): 927-938.

[3] Zuo Jianping, Zhou Hongwei, Liu Yujie. Research on characteristic parameters of sandstone three-point bending failure under different temperatures[J].Chinese Journal of Rock Mechanics

and Engineering,2010,29(4):705-712.
[4] N.A. Al-Shayea, K. Khan, S.N.Abduljauwad. Effects of confining pressure and temperature on mixed-mode (I–II) fracture toughness of a limestone rock[J]. International Journal of Rock Mechanics and Mining Sciences. 2000, 37(4): 629-643.
[5] Naser A. Al-Shayea. Crack propagation trajectories for rocks under mixed mode I－II fracture[J]. Engineering Geology, 2005, 81(1): 84-97.
[6] Xie Hai feng, Rao Qiu hua, Xie Qiang,et al. Plane shear (Mode Ⅱ) fracture experiment analysis of brittle rock at high temperature[J].The Chinese Journal of Nonferrous Metals,2008,18(8):1534-1540.
[7] Kang Jian, The rock thermal fracture research and application[M]. Dalian: Dalian University of Technology Press,2008.
[8] Li Liyun, Wong R H C, Han Zhichao, et al. Experimental and theoretical analysis of three-dimensional surface crack propagation[J]. Chinese Journal of Rock Mechanics and Engineering, 2012,31(2):311-318.
[9] Li Liyun, Xu Fengguang, Xie Heping,et al. Fracture Study on Mode I-III Crack of Rock[J]. Key Engineering Materials, 2006, 325(2): 1217-1220.
[10] He Qingzhi，Li Zhengneng. Engineering fracture mechanics[M]. Beijing：Beijing University of Aeronautics and Astronautics Press, 1993.
[11] Li Shiyu, Yin Xiangchu. Rock fracture mechanics[M].China University of Science and Technology Hefei: Press,2010.